JOURNAL OF AGRICULTURAL AND FOOD CHEMISTRY

ARTICLE

pubs.acs.org/JAFC

Effect of Organic-Phase Solvents on Physicochemical Properties and Cellular Uptake of Astaxanthin Nanodispersions

Navideh Anarjan,[†] Chin Ping Tan,[*,†,‡] Tau Chuan Ling,[§] Kwan Liang Lye,[∥] Hoda Jafarizadeh Malmiri,[⊥] Imededdine Arbi Nehdi,[‡] Yoke Kqueen Cheah,[∥] Hamed Mirhosseini,[†] and Badlishah Sham Baharin[†]

[†]Department of Food Technology, Faculty of Food Science and Technology, Universiti Putra Malaysia (UPM), 43400 UPM, Serdang, Selangor, Malaysia

[‡]Department of Chemistry, College of Science, King Saud University, Riyadh 1145, Saudi Arabia

[§]Institute of Biological Sciences, Faculty of Science, University of Malaya, 50603 Kuala Lumpur, Malaysia

[∥]Department of Biomedical Science, Faculty of Medicine and Health, Universiti Putra Malaysia (UPM), 43400 UPM, Serdang, Selangor, Malaysia

[⊥]Department of Food Science, Faculty of Food Science and Technology, Universiti Putra Malaysia (UPM), 43400 UPM Serdang, Selangor, Malaysia

ABSTRACT: A simplex centroid mixture design was used to study the interactions between two chosen solvents, dichloromethane (DCM) and acetone (ACT), as organic-phase components in the formation and physicochemical characterization and cellular uptake of astaxanthin nanodispersions produced using precipitation and condensation processes. Full cubic or quadratic regression models with acceptable determination coefficients were obtained for all of the studied responses. Multiple-response optimization predicted that the organic phase with 38% (w/w) DCM and 62% (w/w) ACT yielded astaxanthin nanodispersions with the minimum particle size (106 nm), polydispersity index (0.191), and total astaxanthin loss (12.7%, w/w) and the maximum cellular uptake (2981 fmol/cell). Astaxanthin cellular uptake from the produced nanodispersions also showed a good correlation with their particle size distributions and astaxanthin *trans*/*cis* isomerization ratios. The absence of significant ($p > 0.05$) differences between the experimental and predicted values of the response variables confirmed the adequacy of the fitted models.

KEYWORDS: astaxanthin nanodispersions, organic-phase solvents, physicochemical characteristics, cellular uptake

INTRODUCTION

Astaxanthin is one of the xanthophyll carotenoid pigments found in various aquatic animals, such as shrimp, salmon, and lobster, and in some microalgae. Because of its enormous positive impacts on human health and its biological actions, such as anticancer, anti-aging, and anti-inflammatory effects, protecting cells against oxidative cellular and DNA damage and ultraviolet light effects, reducing low-density lipoprotein (LDL)−cholesterol and ulcer symptoms, and boosting the immune system, T-cell production, and cytokine release, it can be incorporated into different food, pharmaceutical, and cosmetic product formulations.[1−3] However, as with many carotenoids, the bioavailability of astaxanthin is often low because of its insolubility in water. While it was believed that the formulation of carotenoids into an oily matrix may provide high bioavailability,[4] it has been shown that the bioavailability of carotenoids from fatty food formulations is not as high as expected. For example, lycopene and capsaicin bioavailabilities in tomato oleoresin and red pepper oleoresin, respectively, are less than other carotenoid-based food formulations, such as tomato and paprika juices.[3]

Water-based carotenoid nanoparticles (nanodispersions) have received considerable interest in recent years because of their high solubility, stability, and bioavailability and their easy applicability to different products compared to their macroscopic crystalline states.[5,6] Nanodispersion systems can be obtained in two ways, by mechanical milling or a precipitation and condensation process; however, milling processes are generally not suitable for the production of nanodispersion systems because, at decreasing particle size, it becomes progressively more difficult to apply mechanical energy without simultaneously inducing particle agglomeration.[6,7] In contrast, precipitation and condensation processes begin with a molecular solution of the active compound in a suitable solvent, followed by homogenization or precipitation in water-containing emulsifiers or biopolymers as surface-active agents and stabilizers, and end with the removal of the unwanted solvents. This process not only allows for the preparation of fine particulate dispersions but also is a relatively easy, cheap, continuous, and controllable method of production that makes it attractive from economical and industrial viewpoints.[6] On the basis of the type of solvent used, the methods can be differentiated into three main process types, namely, emulsification−evaporation, solvent−displacement, and emulsification−diffusion, all of which cause a restriction of particle growth to the nanometer range.[6,8]

In the emulsification−evaporation technique, an appropriate lipophilic solvent is used as the dispersed organic phase and particle size reduction takes place during an emulsification in an intermediate stage. The particle size distribution of the resulting emulsion is adjusted mechanically by homogenization.

Received: April 4, 2011
Revised: June 22, 2011
Accepted: July 3, 2011
Published: July 03, 2011

dx.doi.org/10.1021/jf201314u | *J. Agric. Food Chem.* 2011, 59, 8733–8741

The conversion of an emulsion into a dispersion is performed by removing the solvent using evaporation or diffusion procedures. Particle formation takes place in the emulsion droplet during evaporation when a solubility limitation occurs.[6,7,9] In the solvent−displacement process, a hydrophilic solvent is used to dissolve the active compound and particle formation occurs by precipitation according to nucleation and growth or spinodal-phase separation at extremely high supersaturation conditions. The solvent is removed by evaporation or diffusion as in the former method.[6,8,10] With the use of amphiphilic solvents or solvent mixtures, known as the emulsification−diffusion method, nanoparticle formation takes place through a transient emulsion phase, which forms spontaneously and is then transformed into nanodispersion. In the last two methods, size distribution is controlled by the level of the supersaturation as well as by emulsifier additives, which possibly act as mediators in nucleation, growth, and agglomeration.[6]

Dependent upon the nature of the active compounds in nanodispersions, they can be produced by only one of the mentioned techniques or through all of them, as with most of the carotenoids. Selecting the appropriate solvent and other preparation variables, such as the concentration of bioactive compound, type and concentration of emulsifier(s), and homogenization and evaporation parameters, is the main issue to consider in the preparation of nanodispersions of bioactive compounds with desirable physicochemical characteristics. The latter parameters have been studied in several previous works,[7,9,11−16] but there is currently little knowledge about the effect of solvent type on the characteristics of the resulting nanodispersions.

In present study, the effects of using the three techniques described above for the preparation of aqueous-based astaxanthin nanoparticles were studied by choosing dichloromethane (DCM) as a water-immiscible solvent, acetone (ACT) as a totally water-miscible solvent, and different combinations of these two solvents as a partially water-soluble solvent for the organic phase because of the excellent solubility of astaxanthin in these systems. The proportions of these solvents in the organic phase were then optimized to obtain astaxanthin nanodispersions with the smallest mean particle size, polydispersity index (PDI), and total astaxanthin loss and the highest cellular uptake by HT-29 human colonic epithelial cells.

Sodium caseinate was used as an emulsifier and a stabilizer in the preparation of astaxanthin nanoparticles. During emulsification−diffusion and particle formation, it can be diffused, adsorbed at the interface, and can lower the interfacial tension. Furthermore, it forms a protective interfacial membrane and generates repulsive forces between droplets, because of a combination of electrostatic interactions and hydrophobic interactions; these effects protect the droplets from coalescence. Among surface-active proteins, sodium caseinate is more preferred in the preparation of nanodispersions because of its higher water solubility and thermal stability.[9]

MATERIALS AND METHODS

Materials. *trans*-Astaxanthin (>85%) was donated by Kailu Ever Brilliance Biotechnology Co., Ltd. (Beijing, China). Sodium caseinate, sodium azide, phosphate buffer, analytical- and high-performance liquid chromatography (HPLC)-grade DCM, ACT, methanol, and acetonitrile were provided by Fisher Scientific (Leicestershire, U.K.). HT-29 (HTB 38, human colon carcinoma cell lines) and modified McCoy's 5a medium (ATCC 30-2007) were purchased from the American Type Culture Collection (ATCC, Manassas, VA). Penicillin, streptomycin, fetal bovine serum (FBS), and trypsin 0.25% were obtained from Grand Island Biological Company (GIBCO, Grand Island, NY). Phosphate-buffered saline (PBS) was acquired from Sigma (St. Louis, MO).

Preparation of Aqueous-Based Astaxanthin Nanoparticles. *trans*-Astaxanthin (1%, w/w) was first dissolved in the various selected solvent systems to form an organic dispersed phase. The aqueous (continuous) phase consisted of sodium caseinate (1%, w/w) and sodium azide (0.02%, w/w) dissolved in 0.05 M phosphate buffer (pH 7), was slowly added to the organic phase at an organic/aqueous phase ratio of 1:9 by weight, and homogenized using a conventional homogenizer (Silverson L4R, Buckinghamshire, U.K.) at 5000 rpm for 5 min. The resulting coarse emulsion was then subjected to high-pressure homogenization (APV, Crawley, U.K.) for two passes at 50 MPa. Astaxanthin nanoparticles were produced after the removal of the organic solvent(s) and concentrated 2-fold by rotary evaporation (NE 1001, Eyela, Tokyo, Japan) under reduced pressure at 150 kPa, 47 °C, and 100 rpm. All processing and formulation parameters, except the type of solvent, were held constant during sample preparation.[6,10,11]

Analysis of Mean Particle Size and PDI. The mean particle size and PDI of the astaxanthin nanodispersions were measured with a dynamic light-scattering particle size analyzer (Malvern series ZEN 1600, Malvern Instruments, Ltd., Worcester, U.K.). The experiments were performed on samples diluted (1:10) with deionized water to eliminate multiple scattering effects in the measurements. A laser beam was passed through the samples and scattered in a characteristic pattern based on the particle size. The mean particle size was determined from measurements of scattered light by a photodiode array located behind the cuvette. The PDI was calculated as the best fit between the measured scattered pattern and the one predicted by light-scattering theory.[17] The reported particle size and PDI were calculated from the average of three measurements.

Determination of Astaxanthin Content. Bond Elut C18 cartridges (Varian, Harbor City, CA) were conditioned by washing with 1 mL of methanol and then with 2 mL of deionized water prior to use. A total of 1 mL of sample was applied to the conditioned Bond Elut C18 cartridge. The cartridge was then washed twice with 4 mL of deionized water followed by elution with ACT, and then 2 mL of eluate was further filtered with a membrane filter. An aliquot (20 μL) of filtrate was injected into HPLC.[11]

HPLC analysis was performed using an Agilent liquid chromatography system (Agilent Technologies 1200 Series, Waldbronn, Germany), equipped with a G13150 diode array detector and a Nova-Pak C18 (3.9 × 300 mm) Waters HPLC column, using an isocratic mobile phase consisting of 85% methanol, 5% dichloromethane, 5% acetonitrile, and 5% water. The flow rate was set at 1.0 mL/min, and the injection volume was 20 μL. The chromatogram was recorded from 250 to 700 nm. Peaks were measured at the wavelength of 480 nm.[18] The isomers of astaxanthin were identified according to their retention times and spectra by photodiode array detection.[19] The calibration of the peak area versus astaxanthin concentration was linear in the measured concentration range (R^2 = 0.9943; n = 5).

***In Vitro* Tests of Carotenoid Uptake.** For the *in vitro* tests, the human colon carcinoma HT-29 cell line was used as a model for human colon epithelial cells. Cells were maintained in McCoy's 5a medium (supplemented with L-glutamine and sodium bicarbonate), with 1% (v/v) each of penicillin and streptomycin and 10% (v/v) FBS, at 37 °C in a humidified atmosphere of 95% air and 5% CO_2. At 3 days after seeding, the cells were washed with PBS and incubated with cell culture medium supplemented with 10 μM of the different prepared astaxanthin nanodispersions.[20] After an additional 48 h of incubation with the supplemented culture medium at maintenance conditions (37 °C and 95% air and 5% CO_2), cell monolayers were washed 3 times with PBS and detached by trypsinization; after resuspension in 10 mL of culture

Table 1. Matrix of the Simple Centroid Mixture Design and Experimental Response Values[a]

sample number	DCM (x_1, %)	ACT (x_2, %)	particle size (nm)	PDI	*trans*/9-*cis* isomerization of astaxanthin (%)	*trans*/13-*cis* isomerization of astaxanthin (%)	total astaxanthin loss (%)	cellular level of astaxanthin (fmol/cell)
1	100	0	116.37 ± 4.01	0.242 ± 0.036	11.93 ± 1.55	12.15 ± 0.66	13.09 ± 1.78	2092 ± 168
2	75	25	127.48 ± 3.84	0.178 ± 0.020	3.05 ± 2.71	10.89 ± 1.30	10.47 ± 0.96	1579 ± 75
3	50	50	115.58 ± 4.68	0.177 ± 0.019	2.80 ± 1.88	9.53 ± 0.71	12.24 ± 0.82	2231 ± 147
4	25	75	105.97 ± 3.81	0.203 ± 0.021	2.28 ± 2.20	8.28 ± 1.05	13.83 ± 1.19	3272 ± 69
5	0	100	158.79 ± 0.68	0.186 ± 0.007	2.15 ± 2.29	11.10 ± 1.10	24.02 ± 0.68	923 ± 286

[a] Values are the mean ± standard deviation.

Table 2. Regression Coefficients, R^2, Adjusted R^2, and Probability Values for the Final Reduced Models (Component Proportions)

regression coefficient[a]	average particle size (nm)	PDI	*trans*/9-*cis* isomerization of astaxanthin (%) (g/100 g)	*trans*/13-*cis* isomerization of astaxanthin (%)	total astaxanthin loss (%)	cellular uptake of astaxanthin (fmol/cell)
b_1	115.873	0.2425	11.78	12.096	13.32	2135
b_2	158.293	0.1865	2.84	11.046	23.41	966
b_{12}	−97.939	−0.1383	−21.62	−9.451	−29.03	3752
$(b_{12})^-$	227.911	−0.2827	−19.72	11.120		−12147
R^2	0.9637	0.7743	0.9029	0.7167	0.9089	0.9281
R^2 (adj)	0.9538	0.7127	0.8765	0.6394	0.8937	0.9085
regression						
p value	0.000[b]	0.001[b]	0.000[b]	0.002[b]	0.000[b]	0.000[b]
F value	97.42	12.58	34.11	9.27	59.84	47.35
linear (x_1,x_2)						
p value	0.000[b]	0.001[b]	0.000[b]	0.215	0.000[b]	0.000[b]
F value	158.8	20.22	62.10	1.73	69.40	33.63
quadratic (x_1x_2)						
p value	0.000b	0.004[b]	0.000[b]	0.002[b]	0.000[b]	0.000[b]
F value	92.59	13.48	39.75	15.37	50.29	37.89
full cubic $(x_1x_2)^-$						
p value	0.000b	0.003[b]	0.014[b]	0.039[b]		0.000[b]
F value	128.93	14.49	8.51	5.47		102.11
lack of fit						
p value	0.079	0.666	0.125	0.453	0.081	0.4
F value	3.84	0.20	2.8	0.61	3.27	0.14

[a] b_i, b_{ij}, and (b_{ij}) are the linear, quadratic, and cubic interactions of organic-phase components, respectively. 1, DCM; 2, ACT. [b] Significant ($p < 0.05$).

media, an aliquot of the suspension was used for the determination of the cell number. The remaining cell suspension was washed twice with PBS and then resuspended in 2 mL of water/ethanol (1:1, v/v). The cellular astaxanthin was extracted 3 times with DCM/methanol (1:1, v/v) from cell suspensions,[21] applied to Bond Elut C18 cartridges, and quantified by reverse-phase HPLC.

Transmission Electron Microscopy (TEM) Analysis. The nanodispersions were also observed by TEM for microstructure and particle-size distribution. The sample was prepared using the conventional negative-staining method. TEM images were then taken using an electron microscope (Hitachi H-7100, Nissei Sangyo, Tokyo, Japan) operating at 100 kV.

Experimental Design and Statistical Analysis. A mixture design of the experiment was used to obtain the optimum organic-phase composition, yielding the most desirable nanodispersion characteristics (minimum particle size, PDI, total astaxanthin loss, and maximum cellular uptake), and to investigate the presence of either the synergistic or antagonistic effect in the blends of components. The mixture design is a special case of response-surface design, in which the factors are the components of a blend and the responses are assumed to depend upon only the relative proportions of the blend components but not the amount of the blend itself.[22] An augmented simplex-centroid design was used for the mixture experiments in the present study. In this design, each component was studied at five levels, namely, 0 (0%), $^1/_4$ (25%), $^1/_2$ (50%), $^3/_4$ (75%), and 1 (100%), depending upon the number of components (Table 1). To allow for error estimation, all blends were prepared in three independent replications. Mixture regression analysis was performed to determine the coefficients and significance of the model terms and the coefficients of determination (R^2).

The significance of the estimated regression coefficient for each response variable was assessed by its *F* value at a probability (p) of 0.05. The adequacy of the response models was determined using model analysis, i.e., coefficient-of-determination (R^2) and lack-of-fit analyses.[23] The experimental design matrix, data analysis, and optimization procedure were performed using the Minitab version 14 statistical package (Minitab, Inc., State College, PA). Numerical optimization was

performed with the response optimizer in the Minitab software to determine the exact optimum values of individual and multiple responses resulting in the desired goals.[11] A measure of how the solution has satisfied the combined goals for all responses is known as total desirability. The values for total desirability range from 0 to 1, in which 1 represents the ideal case and 0 indicates that some responses are outside of their acceptable ranges. The adequacy of the models was verified by comparing the experimental data to that predicted by the final models for the optimum astaxanthin nanodispersion using the proportions of solvents recommended by the optimization procedure.

RESULTS AND DISCUSSION

Fitting the Initial Response-Surface Models. Mixture analysis provided empirically significant ($p < 0.05$) models for estimating the variation of the mean particle size, PDI, total astaxanthin loss, and cellular uptake as functions of solvent proportions in the organic phase. The non-significant ($p > 0.05$) terms were dropped from the initial model, and the data were refitted to obtain the final reduced models.

Table 2 contains the coefficients, corresponding R^2 and adjusted R^2 values of the regression equations for the responses, and the corresponding F ratio and p value of each term in the equations. The mixture analysis indicated that the relationships of the organic-phase components, namely, DCM (x_1) and ACT (x_2), with mean particle size, PDI, and astaxanthin cellular uptake could be explained by significant ($p < 0.05$) full cubic polynomial regression models, whereas total astaxanthin loss was predicted by a quadratic regression equation. Relatively high coefficients of determination (R^2), from 0.7743 to 0.9637, were obtained for the regression models, confirming their suitability for the prediction of the studied responses based on organic-phase components (Table 2).

Mean Particle Size and PDI. Generally, in the preparation of astaxanthin nanoparticles during precipitation reactions, nucleation must take place at the highest level of supersaturation during the evaporation or precipitation of the organic phase. To increase the nucleation rate and, consequently, decrease the particle growth, a rapid reduction in supersaturation is required, along with the prevention or control of the agglomeration of the primary particles by the use of specific growth inhibitors, stabilizers, and emulsifiers.[6] The type of organic phase is one of the parameters that can influence all of the mentioned stages by affecting the solubility and diffusion of system components. As shown in Figure 1a, using a water-immiscible solvent (DCM) or a totally water-miscible solvent (ACT) individually or in combination led to the production of nanodispersions with different particle size distributions. The variations of the mean particle size and PDI were significantly ($p < 0.05$) explained by a full cubic regression equation, yielding regression coefficients (R^2) of 0.9637 and 0.7743, respectively (Table 2 and Figure 1a).

The negative quadratic effects of organic-phase components ($x_1 \times x_2$) (Table 2) in the fitted model for the mean particle size and PDI indicated that the components were antagonistic. In other words, using a mixture of these solvent components could decrease the particle size and PDI compared to using them individually. As shown in Table 2 and panels a and b of Figure 1, the full cubic interaction effects of the components were also positively significant on the mean particle size and negatively significant ($p < 0.05$) on PDI variation, meaning that a third-order regression model is suitable for these responses. Thus, there would be both maximum and minimum values for the mean particle size and PDI using combinations of these solvents as the organic phase in different proportions ranging from 0 to 100. The opposite signs of the cubic interactions for the particle size and PDI showed the opposing effect of each component proportion on the variations in these responses; for example, high proportions of DCM in the organic-phase mixture led to the production of astaxanthin nanodispersions with higher particle size and smaller PDI, the opposite of using higher proportions of ACT in the mixture.

The nanoparticle formation takes place when the stabilizer, with a sufficient protective effect, remains at the liquid−liquid interface through the diffusion process. Because the particle formation takes place after solvent diffusion, the size of nanoparticles depends upon the stability of the emulsion droplets, which collide and coalesce.[24] Thus, when using DCM individually as the organic-phase solvent, nearly every formulation resulted in significant aggregation because of its immiscible nature with water and the stabilizer was not able to completely prevent the aggregation of emulsion droplets, leading to a large mean particle size (195.5 nm). In contrast, when only ACT was used as the water-miscible organic phase, after mixing the phases, rapid diffusion of the emulsifier component first led to a reduction in the particle size in the intermediate emulsion that was formed according to the Marangoni effect. ACT diffusion then caused a collapse of the emulsifier in the boundary layer, accompanied by astaxanthin condensation in ACT. Thus, the particles were formed by boundary layer turbulence during solvent diffusion,[6] and in this case, fine emulsions could not be formed as a result of the rapid precipitation of astaxanthin and incomplete absorption of emulsifier onto the freshly produced particles because of their insufficient contact time.[6,24] The fraction of solvent remaining in the precipitation medium could also increase the risk of particle growth by Ostwald ripening, especially because the apparent solubility of mesoscopic systems increases with a decreasing particle size. This consideration applies particularly to particles with an amorphous solid structure.[6]

The results indicated that astaxanthin nanodispersions produced with DCM had smaller mean particle sizes and higher PDI compared to those produced with ACT. Tuning their proportions and using them together may improve the particle size characteristics of the prepared nanodispersions and produce nanodispersions with more desirable properties. Therefore, the solvent proportions in the organic-phase mixture may control the solvent diffusion in the aqueous phase, the solubility of active compound and stabilizer, and the interfacial characteristics of the system.[6] Thus, the minimum particle size and PDI can be obtained by enhancing the ability for rapid and maximum nucleation, the controlled particle growth, the prevention of coalescence, and the low interfacial tension between aqueous and organic phases with optimized solvent proportions, resulting from their partially water-soluble natures.[24]

The single response optimization obtained with Minitab indicated that the organic-phase compositions of 33% DCM (67% ACT) and 65% DCM (35% ACT) would yield astaxanthin nanodispersions with the minimum particle size (105 nm) and PDI (0.173), respectively.

Astaxanthin Loss (%). Astaxanthin initially added to the organic phase was found to be a mixture of approximately 88.4 ± 3.45% *trans*-astaxanthin, 10.1 ± 1.06% 13-*cis*-astaxanthin, and 2.5 ± 0.15% 9-*cis*-astaxanthin according to the HPLC results. During the preparation of nanodispersions, *trans*-astaxanthin is readily interconverted to 9-*cis*- and 13-*cis*-astaxanthin because of steric and thermodynamic driving forces.[19]

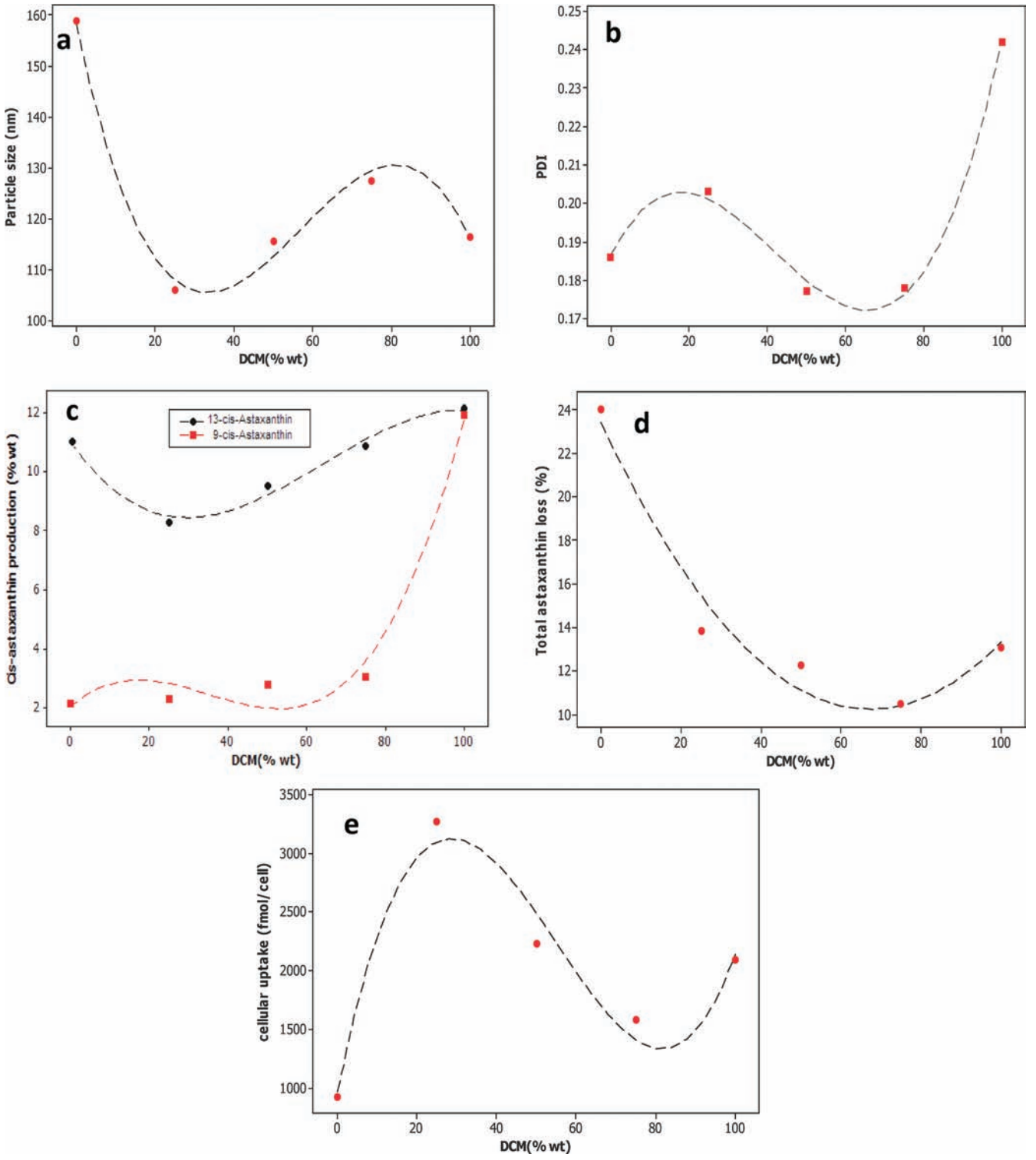

Figure 1. Effect of different DCM compositions of the organic phase on characteristics of astaxanthin nanodispersions: (a) mean particle size, (b) PDI, (c) *cis*-astaxanthin production, (d) total astaxanthin loss, and (e) cellular level of astaxanthin.

The results indicated that the relative contents of *trans*-, 9-*cis*-, and 13-*cis*-astaxanthin in the prepared nanodispersions were different when using different solvents. The 13-*cis* isomerization prevailed over the 9-*cis* isomerization in most of the nanodispersions.

The isomerization of *trans*-astaxanthin into *cis* forms in nanodispersions prepared using pure DCM was higher than in those using pure ACT. Similar results have also been reported in previous studies.[19,25] In the system with pure DCM as the organic phase, the maximum *trans* to *cis* isomerization percentage was found to be 24% and the contents of the 9-*cis* and 13-*cis* isomers were almost equal. As shown in Table 2 and Figure 1c, the regression models for the *trans* to 9-*cis* and the *trans* to 13-*cis*

isomerizations of astaxanthin in the nanodispersions were found to be full cubic (third-order) equations. Using the response optimizer, the minimum 9-*cis* and also 13-*cis* isomer productions were predicted to occur in 30% DCM (70% ACT) and 50% DCM (50% ACT), respectively, and the maximum conversions were predicted to occur in 100% DCM, as mentioned above. Thus, the minimum *trans* to *cis* isomerizations were predicted to occur when a solvent mixture (i.e., the solvent-diffusion technique) was used.

The total astaxanthin concentration showed a decrease during the processing steps in all samples. It is well-known that astaxanthin, similar to other carotenoids, is very sensitive to light, oxygen, heat, and different active agents, such as free radicals.[26] The possible cavitation during homogenization may cause the production of free radicals that would trigger a loss of astaxanthin in all of the nanodispersions.[27] *trans*-Astaxanthin loss thus likely occurred because of both isomerization and degradation. The variation of total astaxanthin loss was significantly ($p < 0.05$) explained by a quadratic regression equation ($R^2 = 0.9089$) (Table 2 and Figure 1d). The negative quadratic effects of the solvent components ($x_1 \times x_2$) in the fitted model for astaxanthin loss pointed to their antagonistic binary combinations. Therefore, the use of mixed solvents could produce nanodispersions with low total astaxanthin loss (%) compared to the use of a pure solvent as the organic phase. The predicted second-order regression model for total astaxanthin loss meant that there was an optimum component percentage in the solvent mixture leading to minimum astaxanthin loss, which was 68% DCM and 32% ACT as predicted by the single response optimizer. The corresponding astaxanthin loss (%) for this mixture was calculated to be 10%.

The minimum astaxanthin loss with the use of mixed solvents was obtained in nanodispersions with approximately the maximum mean particle size. This result concurs with those of previous researchers.[11,16,28] The larger surface area of astaxanthin in nanodispersions with a smaller mean particle size can significantly reduce the chemical stability of astaxanthin nanodispersions by providing more contact surface area between astaxanthin particles and the aqueous environment.[7]

The nanodispersions produced using ACT alone as the organic phase showed higher astaxanthin loss compared to those produced with pure DCM. This result may be related to the hydrophobic nature of DCM and the hydrophilic nature of ACT. When DCM is used as the organic phase, the active radicals occurring in the system (that are mostly ionic in nature) were repelled and could not easily reach astaxanthin, whereas when using ACT, oxygen and other reagents could easily diffuse into this organic phase and cause high astaxanthin loss because of their easier contact with carotenoid molecules. Furthermore, the higher boiling point of ACT compared to DCM could cause more astaxanthin loss in ACT dispersion systems because of its higher latent heat of vaporization and, consequently, longer exposure to high temperatures during evaporation and the solvent removal process.

Cellular Uptake. Food emulsion and dispersion designs aimed at delivering lipophilic bioactive compounds should include an estimate of their bioavailability to support the claimed effect.[3] For absorption of a carotenoid, it needs to be released from the food matrix, transferred into lipid conveyers, integrated with mixed bile salt micelles during digestion, undergone possible metabolism by enterocytes, and incorporated into chylomicrons (CMs) to secrete into the lymph.[29] The dissolution rate, hydrophilicity, particle size, surface area, *cis* or *trans* isomerization, and polymorphism are some of the important factors affecting the cellular uptake of carotenoids.[30] Whereas the direct evaluation of carotenoid absorption in human or animal models suffers from considerable limitations in the design and high cost of labor and equipment, thus prohibiting the systematic screening of various food sources, processing methods, and other dietary factors,[29,30] *in vitro* models, such as cellular uptake measurements, have been of great interest because of their potential to provide useful insights about the relative bioavailability of carotenoids and the effects of different parameters on the potential bioavailability and the bioaccessibility of ingested carotenoids. *In vitro* models are relatively inexpensive and technically simple; standard laboratory equipment is sufficient. The high-throughput potential facilitates the screening of numerous samples, and the experiments are readily controlled for the investigation of mechanisms.[30,31]

Table 3. Regression Coefficients, R^2, Adjusted R^2, and Probability Values for the Regression Equation Predicting Astaxanthin Cellular Uptake (fmol/Cell) Variation with the Mean Particle Size (nm), PDI, and *trans* to 9-*cis* and 13-*cis* Isomerizations (%, w/w) of Astaxanthin in Astaxanthin Nanodispersions

predictors	regression coefficients	*F* value	*p* value
constant	4725.30	83.72	0.000[a]
mean particle size (nm)	−24.38	79.39	0.000[a]
PDI	16311.00	52.71	0.000[a]
trans to 9-*cis* isomerization	−55.42	5.24	0.045[a]
trans to 13-*cis* isomerization	−252.49	28.62	0.000[a]
R^2	0.987		
R^2 (adj)	0.981		

[a] Significant ($p < 0.05$).

In this work, the cellular uptake of astaxanthin from nanodispersions was investigated using colon carcinoma cells (HT-29) as a model for human colon epithelial cells. These cells are able to form and secrete CMs, large lipoproteins rich in triglycerides that are required for *in vivo* intestinal absorption of fat-soluble nutrients, such as carotenoids. The differentiation process in HT-29 cells is apparently similar to that observed during the embryonic development of the intestine.[32]

Table 2 and Figure 1e show the results for the cellular uptake by the HT-29 cell line of astaxanthin nanodispersions prepared with different organic-phase compositions. The variation of the cellular uptake of astaxanthin with organic-phase composition proportions was significantly ($p < 0.05$) predicted by a full cubic regression model ($R^2 = 0.9281$). The positive quadratic and negative full cubic effects of solvent components in the fitted model indicated their synergistic binary and antagonistic ternary interaction effects, meaning that both the highest and lowest cellular uptake of astaxanthin would be obtained using combinations of DCM and ACT. Low concentrations of DCM in the mixed solvents would produce nanodispersions with higher cellular uptake, but the nanodispersions produced with only DCM showed higher cellular uptake than those with only ACT. According to the individual response optimization, the highest cellular uptake of astaxanthin was predicted to be produced using 31% DCM and 61% ACT.

Table 3 shows the regression equation and probability values of the fitted model for the variation in cellular uptake of astaxanthin with the mean particle size, PDI, and *trans* to 9-*cis* and 13-*cis* isomerizations in the various nanodispersions. The

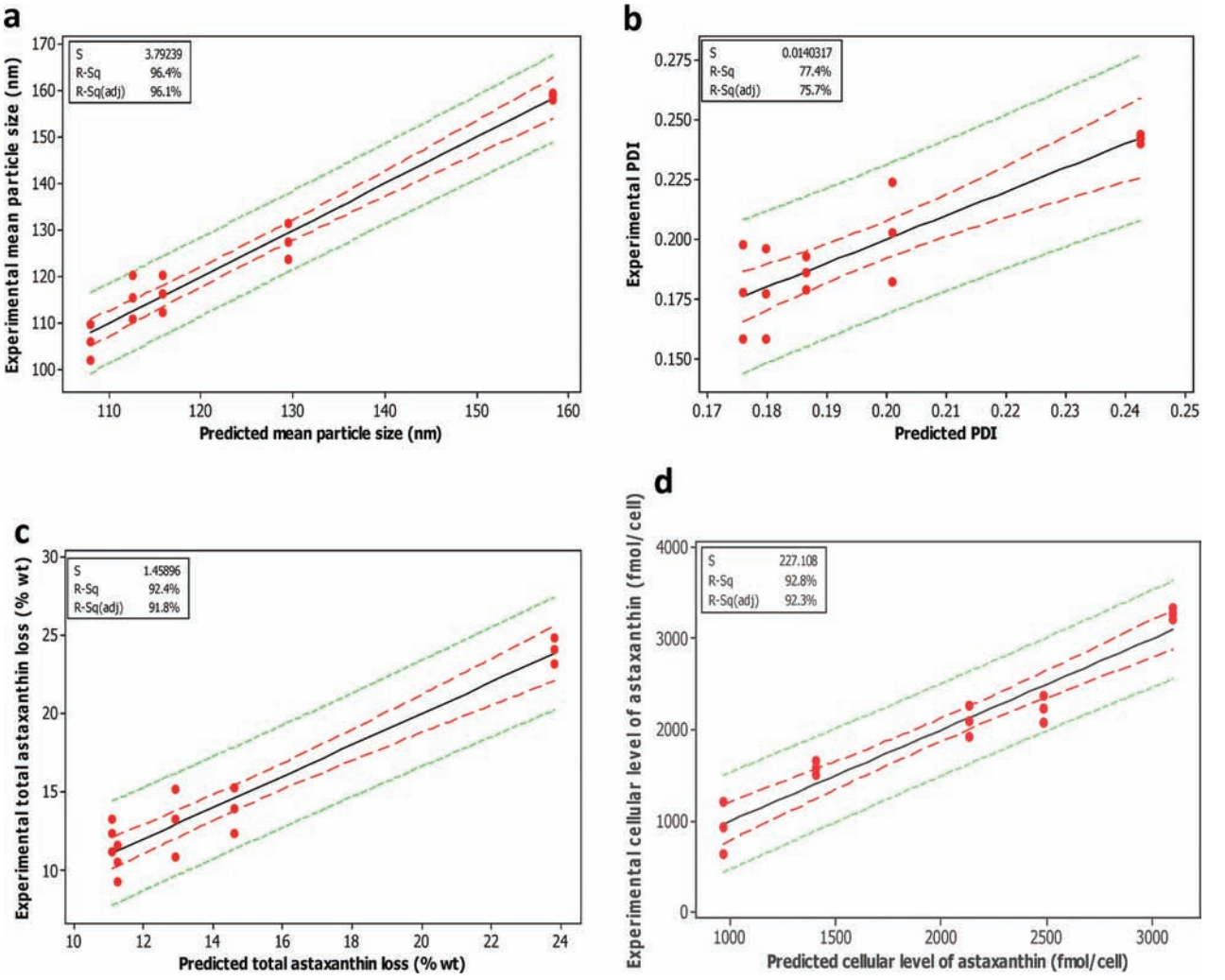

Figure 2. Fitted line plots between the experimental and predicted values of studied responses.

high coefficient of determination ($R^2 = 0.987$) obtained for this regression model confirmed the close correlation between the cellular uptake and other studied responses. The cellular uptake of astaxanthin increased with a decreasing particle size and *trans* to *cis* isomerization and with an increasing PDI. The mean particle size of the nanodispersions showed the highest significant effect (i.e., the lowest p value and highest F value) compared to the other predictors. Between the *cis* isomerizations of astaxanthin, the degree of 13-*cis* isomerization affected the variation of cellular uptake of astaxanthin from nanodispersions more than the 9-*cis* isomerization. The inverse dependence of cellular uptake upon the particle size and *trans* to *cis* isomerizations of astaxanthin was expected according to several theoretical *in vivo* dissolution models[33,6] and previously reported results.[19,32,34] However, the exact cause of the changes in cellular uptake with PDI remains unexplained.

Optimization and Validation Procedures for the Optimum Processing Condition. In the present study, an astaxanthin nanodispersion would be considered an optimum product if it possessed the smallest mean particle size, the narrowest PDI, the least total astaxanthin loss, and the highest cellular uptake. The numerical multiple optimizations showed that the most desirable astaxanthin nanodispersion was predicted to be obtained with the use of an organic phase with 38% DCM and 62% ACT. At this optimum organic-phase ratio, the corresponding predicted response values for the mean particle size, PDI, total astaxanthin loss, and cellular uptake were predicted to be 106 nm, 0.191, 12.7%, and 2981 fmol/cell, respectively, for a total desirability of 0.8213.

As shown in Figure 2, the overall closeness between the predicted and experimental values of the responses confirmed the adequacy of the models. The optimum astaxanthin nanodispersion containing the predicted optimum organic-phase formulation was also prepared in triplicate and evaluated in terms of the studied characteristics. The corresponding experimental values for the mean particle size, PDI, total astaxanthin loss, and cellular uptake of the nanodispersion prepared using the predicted optimum proportions were 110 ± 6.04, 0.201 ± 0.016, $9.9 \pm 3.5\%$, and 3057 ± 96 fmol/cell, respectively. Thus, the absence of significant ($p > 0.05$) differences between the experimental and predicted values reconfirmed the adequacy of the final models employed.

DCM and ACT residues were recorded to be approximately 0.025 ppm in prepared astaxanthin nanodispersions. The residual solvent level was shown to be at an acceptable level according the International Conference on Hormonization (ICH) and

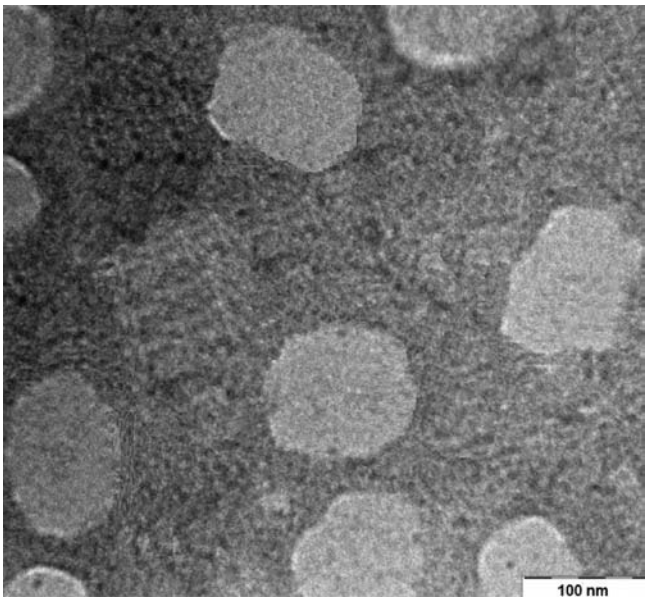

Figure 3. Transmission electron micrograph of optimum astaxanthin nanoparticles in water (optimum astaxanthin nanodispersion).

indicated that the produced nanodispersions can be applied in different food and pharmaceutical formulations.

There was no significant ($p < 0.05$) change in the mean particle size of the resulting optimum astaxanthin nanodispersion over the 8 week storage at 5 °C. Therefore, no occurrence of coalescence was observed in the nanodispersion, and this observation verified the high physical stability of the produced nanodispersions. However, the significant ($p < 0.05$) decrease in the astaxanthin content (35%) of the nanodispersions during storage showed their limited chemical stability.

TEM Analysis. A representative TEM image of the optimum astaxanthin nanodispersion is presented in Figure 3. The optimum formulated astaxanthin nanodispersion contained relatively well-defined but rather polydisperse quasi-spherical-shaped particles, as evidenced from the TEM observation. The observations closely corresponded with the results observed in the dynamic light-scattering particle-size analysis.

CONCLUSION

In this study, the experimental design of mixtures was applied to find empirically significant ($p < 0.05$) models for predicting the variations of the mean particle size, PDI, cellular uptake, *trans* to *cis* isomerizations, and total astaxanthin loss of astaxanthin nanodispersions as a function of organic-phase (solvent) proportions. The results clearly showed that the studied physicochemical and biological properties of the nanodispersions were significantly ($p < 0.05$) influenced by organic-phase compositions depending upon the solubility of the organic phase in water. Concerning the stated goals, the astaxanthin nanodispersion prepared using a mixture of 38% DCM and 62% ACT as the organic phase was shown to possess the optimum characteristics. Thus, an organic phase with a partially water-soluble nature, corresponding to the solvent-diffusion technique, yielded an astaxanthin nanodispersion with a lower mean particle size, PDI, and total astaxanthin loss and a higher cellular uptake than either fully water-insoluble (the emulsification−evaporation technique) or water-soluble (the solvent−displacement technique) solvents.

AUTHOR INFORMATION

Corresponding Author

*Telephone: +603-89468418. Fax: +603-89423552. E-mail: tancp@putra.upm.edu.my.

Funding Sources

Financial support of this work by the Ministry of Science, Technology, and Innovation of Malaysia through Science Fund (05-01-04-SF0384) and the Ministry of Higher Education through Fundamental Research Grant Scheme (02-11-08-0619FR) is gratefully acknowledged.

REFERENCES

(1) Tachaprutinun, A.; Udomsup, T.; Luadthong, C.; Wanichwecharungruang, S. Preventing the thermal degradation of astaxanthin through nanoencapsulation. *Int. J. Pharm.* **2009**, *374*, 119–124.

(2) Guerin, M.; Huntley, M. E.; Olaizola, M. *Haematococcus* astaxanthin: Applications for human health and nutrition. *Trends Biotechnol.* **2003**, *21*, 210–216.

(3) Fernandez-Garcia, E.; Rincon, F.; Perez-Galvez, A. Developing an emulsifier system to improve the bioaccessibility of carotenoids. *J. Agric. Food Chem.* **2008**, *56*, 10384–10390.

(4) Yeum, K. J.; Russell, R. M. Carotenoid bioavailability and bioconversion. *Annu. Rev. Nutr.* **2002**, *22*, 483–504.

(5) Higuera-Ciapara, I.; Felix-Valenzuela, L.; Goycoolea, F. M.; Argüelles-Monal, W. Microencapsulation of astaxanthin in a chitosan matrix. *Carbohydr. Polym.* **2004**, *56*, 41–45.

(6) Horn, D.; Rieger, J. Organic nanoparticles in the aqueous phase—Theory, experiment, and use. *Angew. Chem., Int. Ed.* **2001**, *40*, 4330–4361.

(7) Tan, C. P.; Nakajima, M. β-Carotene nanodispersions: Preparation, characterization and stability evaluation. *Food Chem.* **2005**, *92*, 661–671.

(8) Verma, S.; Burgess, D. Solid nanosuspensions: The emerging technology and pharmaceutical applications as nanomedicine. In *Pharmaceutical Suspensions: From Formulation Development to Manufacturing*; Kulshreshtha, A. K., Singh, O. N., Wall, G. M., Eds.; Springer: New York, 2010; pp 285−318.

(9) Chu, B. S.; Ichikawa, S.; Kanafusa, S.; Nakajima, M. Preparation of protein-stabilized β-carotene nanodispersions by emulsification−evaporation method. *J. Am. Oil Chem. Soc.* **2007**, *84*, 1053–1062.

(10) Leong, W. F.; Man, Y. B. C.; Lai, O. M.; Long, K.; Misran, M.; Tan, C. P. Optimization of processing parameters for the preparation of phytosterol microemulsions by the solvent displacement method. *J. Agric. Food Chem.* **2009**, *57*, 8426–8433.

(11) Anarjan, N.; Mirhosseini, H.; Baharin, B. S.; Tan, C. P. Effect of processing conditions on physicochemical properties of astaxanthin nanodispersions. *Food Chem.* **2010**, *123*, 477–483.

(12) Cheong, J. N.; Tan, C. P.; Man, Y. B. C.; Misran, M. α-Tocopherol nanodispersions: Preparation, characterization and stability evaluation. *J. Food Eng.* **2008**, *89*, 204–209.

(13) Chu, B. S.; Ichikawa, S.; Kanafusa, S.; Nakajima, M. Preparation and characterization of β-carotene nanodispersions prepared by solvent displacement technique. *J. Agric. Food Chem.* **2007**, *55*, 6754–6760.

(14) Ribeiro, H. S.; Chu, B. S.; Ichikawa, S.; Nakajima, M. Preparation of nanodispersions containing β-carotene by solvent displacement method. *Food Hydrocolloids* **2008**, *22*, 12–17.

(15) Tan, C. P.; Nakajima, M. Effect of polyglycerol esters of fatty acids on physicochemical properties and stability of β-carotene nanodispersions prepared by emulsification/evaporation method. *J. Sci. Food Agric.* **2005**, *85*, 121–126.

(16) Yin, L. J.; Chu, B.-S.; Kobayashi, I.; Nakajima, M. Performance of selected emulsifiers and their combinations in the preparation of β-carotene nanodispersions. *Food Hydrocolloids* **2009**, *23*, 1617–1622.

(17) Mirhosseini, H.; Tan, C. P.; Hamid, N. S. A.; Yusof, S. Optimization of the contents of Arabic gum, xanthan gum and orange

oil affecting turbidity, average particle size, polydispersity index and density in orange beverage emulsion. *Food Hydrocolloids* **2008**, *22*, 1212–1223.

(18) Yuan, J. P.; Chen, F. Chromatographic separation and purification of *trans*-astaxanthin from the extracts of *Haematococcus pluvialis*. *J. Agric. Food Chem.* **1998**, *46*, 3371–3375.

(19) Yuan, J. P.; Chen, F. Isomerization of *trans*-astaxanthin to *cis*-isomers in organic solvents. *J. Agric. Food Chem.* **1999**, *47*, 3656–3660.

(20) Briviba, K.; Bornemann, R.; Lemmer, U. Visualization of astaxanthin localization in HT29 human colon adenocarcinoma cells by combined confocal resonance Raman and fluorescence microspectroscopy. *Mol. Nutr. Food Res.* **2006**, *50*, 991–995.

(21) Briviba, K.; Schnäbele, K.; Schwertle, E.; Blockhaus, M.; Rechkemmer, G. β-Carotene inhibits growth of human colon carcinoma cells in vitro by induction of apoptosis. *Biol. Chem.* **2001**, *382*, 1663–1668.

(22) Myers, R.; Montgomery, D. C. *Response Surface Methodology*; Wiley: New York, 2002.

(23) Weng, W. L.; Liu, Y. C.; Lin, C. W. Studies on the optimum models of the dairy product Kou Woan Lao using response surface methodology. *Asian-Australas. J. Anim. Sci.* **2001**, *14*, 1470–1476.

(24) Song, K. C.; Lee, H. S.; Choung, I. Y.; Cho, K. I.; Ahn, Y.; Choi, E. J. The effect of type of organic phase solvents on the particle size of poly(D,L-lactide-*co*-glycolide) nanoparticles. *Colloid Surf., A* **2006**, *276*, 162–167.

(25) Yuan, J. P.; Chen, F. Kinetics for the reversible isomerization reaction of *trans*-astaxanthin. *Food Chem.* **2001**, *73*, 131–137.

(26) Chen, X.; Chen, R.; Guo, Z.; Li, C.; Li, P. The preparation and stability of the inclusion complex of astaxanthin with β-cyclodextrin. *Food Chem.* **2007**, *101*, 1580–1584.

(27) Lander, R.; Manger, W.; Scouloudis, M.; Ku, A.; Davis, C.; Lee, A. Gaulin homogenization: A mechanistic study. *Biotechnol. Prog.* **2000**, *16*, 80–85.

(28) Mao, L.; Xu, D.; Yang, J.; Yuan, F.; Gao, Y.; Zhao, J. Effects of small and large molecule emulsifiers on the characteristics of β-carotene nanoemulsions prepared by high pressure homogenization. *Food Technol. Biotechnol.* **2009**, *47*, 336–342.

(29) Failla, M. L.; Chitchumroonchokchai, C. In vitro models as tools for screening the relative bioavailabilities of provitamin A carotenoids in foods. *Harvest Plus Tech. Monogr.* **2005**, No. Series 3, 1–32.

(30) Failla, M. L.; Huo, T.; Thakkar, S. K. In vitro screening of relative bioaccessibility of carotenoids from foods. *Asia Pac. J. Clin. Nutr.* **2008**, *17*, 200–203.

(31) Ribeiro, H. S.; Guerrero, J. M. M.; Briviba, K.; Rechkemmer, G.; Schuchmann, H. P.; Schubert, H. Cellular uptake of carotenoid-loaded oil-in-water emulsions in colon carcinoma cells in vitro. *J. Agric. Food Chem.* **2006**, *54*, 9366–9369.

(32) During, A.; Hussain, M. M.; Morel, D. W.; Harrison, E. H. Carotenoid uptake and secretion by CaCo-2 cells: β-Carotene isomer selectivity and carotenoid interactions. *J. Lipid Res.* **2002**, *43*, 1086–1095.

(33) Amidon, G. L.; Lennernas, H.; Shah, V. P.; Crison, J. R. A theoretical basis for a biopharmaceutic drug classification: The correlation of in vitro drug product dissolution and in vivo bioavailability. *Pharm. Res.* **1995**, *12*, 413–419.

(34) Ferruzzi, M. G.; Lumpkin, J. L.; Failla, M.; Schwartz, S. J. Digestive stability, micellarization, and uptake of β-carotene isomers by Caco-2 human intestinal cells. *J. Agric. Food Chem.* **2006**, *54*, 2780–2785.